Computational Geosciences
https://doi.org/10.1007/s10596-020-09983-0

ORIGINAL PAPER

Iterative solvers for Biot model under small and large deformations

Manuel Antonio Borregales Reverón[1] · Kundan Kumar[2,3] · Jan Martin Nordbotten[2] · Florin Adrian Radu[2]

Received: 30 May 2019 / Accepted: 3 June 2020

Abstract

We consider L-scheme and Newton-based solvers for Biot model under large deformation. The mechanical deformation follows the Saint Venant-Kirchoff constitutive law. Furthermore, the fluid compressibility is assumed to be non-linear. A Lagrangian frame of reference is used to keep track of the deformation. We perform an implicit discretization in time (backward Euler) and propose two linearization schemes for solving the non-linear problems appearing within each time step: Newton's method and L-scheme. Each linearization scheme is also presented in a monolithic and a splitting version, extending the undrained split methods to non-linear problems. The convergence of the solvers, here presented, is shown analytically for cases under small deformation and numerically for examples under large deformation. Illustrative numerical examples are presented to confirm the applicability of the schemes, in particular, for large deformation.

Keywords Large deformation · Biot's model · L-scheme · Newton's method · Poroelasticity

1 Introduction

The coupling of flow and mechanics in a porous medium, typically called poromechanics, plays a crucial role in many socially relevant applications. These include geothermal energy extraction, energy storage in the subsurface, CO_2 sequestration, and understanding of biological tissues. The increased role played by computing in the development and optimization of (industrial) technologies for these applications implies the need for improved mathematical models in poromechanics and robust numerical solvers for them.

The most common mathematical model for coupled flow and mechanics in porous media is the linear, quasi-stationary Biot model [8–10, 52]. The model consists of two coupled partial differential equations, representing balance of forces for the mechanics and conservation of mass and momentum for (single-phase) flow in porous media.

In terms of modelling, Biot's model has been extended to unsaturated flow [14, 37], multiphase flow [27, 28, 34, 36, 47], thermo-poroelasticity [20], and reactive transport in porous media [33, 48], where nonlinearities arise in the flow model, specifically in the diffusion term, the time derivative term, and/or in Biot's coupling term. The mechanics model can also be extended to the elasto-plastic [3, 56], the fracture propagation [35], and the hyperelasticity [21, 22], where the nonlinearities appear in the constitutive law of the material, in the compatibility condition and/or the conservation of momentum equation. Furthermore, elastodynamics or non-stationary Biot, i.e., Biot-Allard model [38], includes a convolution in the media parameters, like the permeability and/or the mechanical elasticity tensor. In this paper, we are going to explore a general case that allows large deformations. The mechanical deformation follows the Saint Venant-Kirchoff constitutive law and the fluid compressibility in the fluid equation is assumed to be non-linear. This model formulation is needed to later consider extensions of Biot's model to plasticity, more general hyperelastic materials, and elastodynamics.

Finding closed-form solutions for coupled problems is very difficult, and commonly based on various simplifications. We, therefore, resort to numerical approximations. In general, there are two approaches to solve such problems, a monolithic, or fully coupled, and splitting, or weakly coupled scheme. In general, the fully coupled schemes for fluid potential and mechanical deformation are stable, have excellent convergence properties, and ensure that the numerical solution is consistent with the underlying continuous differential equations [29, 55]. Despite obvious

✉ Manuel Antonio Borregales Reverón
manuel.borregales@sintef.no

[1] Mathematics and Cybernetics, SINTEF Digital, PO Box 124 Blinder, Oslo, Norway

[2] Department of Mathematics, University of Bergen, PO Box 7800, Bergen, Norway

[3] Department of Mathematics and Computer Science, Karlstad University, Universitetsgatan 2, 651 88 Karlstad, Sweden

Published online: 18 July 2020

advantages, the monolithic solvers for the fully coupled problem are more difficult to implement, and show difficulties solving the resulting linear system. In the weakly coupled approach, while marching in time, the flow problem (or the mechanics) is time-lagged, thereby decoupling the two problems. Due to the complexities associated with the fully coupled scheme, the industry standard remains to use weakly coupled or iteratively coupled approaches [19, 41, 51, 58]. Weakly coupled schemes, where there are no iterations within a time step, have particularly been questioned in previous works [18, 23, 41, 44]; they have been shown to lack robustness and even convergence, if not properly designed. A splitting approach takes somewhat of a middle path; at each time step, it decouples the flow and mechanics, but iterates so that the convergence is achieved. Undrained and fixed-stress schemes are examples of splitting schemes. However, the main difference between them is that fixed-stress scheme stabilizes the flow problem while the undrained scheme stabilizes the mechanics. In order to ensure the robustness and accuracy of the resulting computations, it is essential to understand the efficiency, stability, and convergence of monolithic and splitting solvers, in particular in the presence of non-linearities.

In this work, we present monolithic and splitting approaches for solving this non-linear system, that is, non-linear compressibility and the Saint Venant-Kirchoff constitutive law for stress–strain relationship. Moreover, we rigorously study the convergence of our solvers, including the Newton-based ones, under the assumption of small deformations. As for the splitting approach, a stabilization term is added in the mechanics equation to ensure convergence, resembling the undrained splitting method (see [31, 39]).

We use linear continuous Galerkin elements for the discretization of the mechanics equation and mixed finite elements for the flow equation [7, 24, 30, 42, 57]. Precisely, the lowest order Raviart-Thomas elements are used [17]. We expect, however, that the solution strategy discussed herein will be applicable to other combinations of spatial discretizations such as those discussed in [40, 49] and the references therein. Backward Euler is used for the temporal discretization.

To summarize, the new contributions of this paper are:

- We propose Newton- and L-scheme-based monolithic and splitting schemes for solving the Biot model under small or large deformation.
- The convergence analyses of all solvers are shown rigorously under the assumption of small deformations.
- The convergence of splitting algorithms is shown through numerical examples for a general non-linear Biot model that includes large deformations.

We mention some relevant works in this direction. For the convergence analysis of the undrained split method applied to the linear Biot model, we refer to [5, 6, 12, 25, 26, 39]. For a discussion on the stabilization/tuning parameter used in the undrained split approach, we refer to [12, 15]. A theoretical investigation on the optimal choice for this parameter is performed in [53]. The linearization is based on either Newton's method, or the L-scheme [37, 43, 47] or a combination of them [14, 37]. For monolithic and splitting schemes based solely on L-scheme, we refer to [11]. Multirate time discretization or higher order space-time Galerkin method has also been proposed for the linear Biot model in [1] and [6], respectively.

The paper is structured as follows. In the next section, we present the mathematical model. In Section 3, we propose four iterative solvers. Section 4 shows the analysis of iterative solvers under the assumption of small deformations. Numerical results are presented in Section 5 followed by the conclusion in Section 6.

2 Governing equations

We consider a fluid flow problem in a poroelastic bounded reference domain $\Omega \subset \mathbb{R}^d$, $d \in \{2, 3\}$ under large deformation. A Lagrangian frame of reference is used to keep track of the invertible transformation $x := \{x(X, t) = X + \mathbf{u}(X, t) : X \in \Omega \to x \in \Omega_t\}$, where Ω_t is the deformed domain at time t and $\mathbf{u}$ represents the deformation field. The gradient of the transformation and its determinant are given by $\mathbf{F} = \nabla x(X, t)$ and $J = \det(\mathbf{F})$. All differentials are with respect to the undeformed coordinates X, unless otherwise stated. We summarize in Table 1 the list of symbols herein used.

We will now write the conservation of momentum and mass equation in Ω. The conservation of momentum represents the balance between the first Piola-Kirchhoff poroelastic stress $\mathbf{\Pi}$ in Ω and the forces acting on Ω_t, and is given by:

$$-\nabla \cdot \mathbf{\Pi} = \rho_b \mathbf{g}, \tag{1}$$

where $\rho_b = J\varrho_b$ is the bulk density in Ω, ϱ_b is the bulk density in Ω_t, and $\mathbf{g}$ is gravity.

We exploit the relation $\mathbf{\Pi} = \mathbf{F}\mathbf{\Sigma}$ since the constitutive laws are developed for the second Piola-Kirchhoff poroelastic stress $\mathbf{\Sigma}$. This stress tensor is composed of the effective mechanical stress $\mathbf{\Sigma}^{eff}$ and the pore pressure p by the following relation:

$$\mathbf{\Sigma} = \mathbf{\Sigma}^{eff} - J\mathbf{F}^{-1}\mathbf{F}^{-\top} p,$$

where $J\mathbf{F}^{-1}\mathbf{F}^{-\top}$ ensures that pressure p exerts an isotropic stress in Ω_t. We assume an isotropic poroelastic material with constant shear modulus μ and a non-linear function

Table 1 Nomenclature

Parameters			
First Piola-Kirchhoff poroelastic stress	$\mathbf{\Pi}$	Displacement	$\mathbf{u}$
Second Piola-Kirchhoff poroelastic stress	$\mathbf{\Sigma}$	Mass flux	$\mathbf{q}$
Second Piola-Kirchhoff effective stress	$\mathbf{\Sigma}^{\mathbf{eff}}$	Pressure	p
Green strain tensor	$\mathbf{E}$	Fluid density	ρ_f
Transformation's gradient	$\mathbf{F}$	Bulk density	ϱ_b
Transformation's determinant	J	Source term	S_f
Lamé's first parameter	λ	Biot's constant	α
Lamé's second parameter	μ	Biot's modulus	M
Kinematic fluid viscosity	ν_f	Fluid content	Γ
Lagrangian permeability tensor	$\mathbf{K}$	Lagrangian gravity	$\mathbf{G}$
Eulerian permeability tensor	$\mathbf{k}$	Eulerian gravity	$\mathbf{g}$
Poroelastic stress tensor	$\boldsymbol{\sigma}^{por}$	Effective stress tensor	$\boldsymbol{\sigma}$
Body forces	$\boldsymbol{f}$	Time step counter	n
Linearized strain tensor	ε	Iterative counter	i
Incremental operator	δ	Mesh size	h
Partial derivate operator	∂	Time step size	τ

of the volumetric strain $\mathfrak{c}(\cdot)$ [11, 54]. The effective stress is given by Saint Venant-Kirchhoff constitutive law: $\mathbf{\Sigma}^{\mathbf{eff}} = \mathbf{2}\mu\mathbf{E} + \mathfrak{c}\,(\mathrm{tr}(\mathbf{E}))$, where the Green strain tensor $\mathbf{E}$ is defined by:

$$\mathbf{E} = \frac{1}{2}\left(\boldsymbol{\nabla}\mathbf{u} + \boldsymbol{\nabla}^{\top}\mathbf{u} + (\boldsymbol{\nabla}\mathbf{u})^{\top}\boldsymbol{\nabla}\mathbf{u}\right).$$

The conservation of fluid mass is given by:

$$\dot{\Gamma} + \boldsymbol{\nabla}\cdot\mathbf{q} = S_f. \tag{2}$$

We consider a fluid mass $\Gamma = J\rho_f\phi$ of a slightly compressible fluid, where ϕ is the porosity in Ω_t and ρ_f the fluid density and S_f the source term in Ω respectively. The mass flux is given by $\mathbf{q} = \rho_{f,ref}\mathbf{q}_v$, where $\rho_{f,ref}$ is the reference density of the fluid and $\mathbf{q}_v$ is the first Piola transform of the corresponding volumetric flux in Ω_t. The time derivative of the fluid content $\dot{\Gamma} = \dot{\Gamma}(\mathbf{u}, p)$ is considered to be a function of the pressure and the pore volume change due to the deformation field. We consider Darcy's law:

$$\mathbf{q}_v = -\frac{1}{\rho_{f,ref}}\mathbf{K}(\boldsymbol{\nabla}\mathbf{u})\left(\boldsymbol{\nabla}p - \rho_{f,ref}\mathbf{G}\right), \tag{3}$$

where $\mathbf{K} = J\mathbf{F}^{-1}\mathbf{k}\mathbf{F}^{-\top}$ is the corresponding transformation of the mobility tensor $\mathbf{k}$ in Ω_t and $\mathbf{G}{=}\mathbf{F}^{\top}\mathbf{g}$. Finally, the general non-linear Biot model considered in this paper reads as:

Find $(\mathbf{u}, \mathbf{q}, p)$ such that:

$$\begin{aligned} -\boldsymbol{\nabla}\cdot\mathbf{\Pi}\,(\boldsymbol{\nabla}\mathbf{u}, p) &= \rho_b\mathbf{g}, && \text{in } \Omega\times]0,T[,\\ \mathbf{q} &= -\mathbf{K}(\boldsymbol{\nabla}\mathbf{u})\left(\boldsymbol{\nabla}p - \rho_{f,ref}\mathbf{G}(\boldsymbol{\nabla}\mathbf{u})\right), && \text{in } \Omega\times]0,T[,\\ \dot{\Gamma}(\mathbf{u}, p) + \boldsymbol{\nabla}\cdot\mathbf{q} &= S_f, && \text{in } \Omega\times]0,T[. \end{aligned} \tag{4}$$

To complete the model, we consider Dirichlet boundary conditions (BC) and initial conditions given by $(\mathbf{u}_0, p_0)$ such that $\Gamma(\mathbf{u}_0, p_0) = \Gamma_0$ and $\mathbf{\Pi}(\mathbf{u}_0, p_0) = \mathbf{\Pi}_0$ at time $t = 0$. The functions Γ_0 and $\mathbf{\Pi}_0$ are supposed to be given (and to be sufficiently regular).

In practice, the initial data $\mathbf{u}_0$ and p_0 are not independent and can be obtained by solving the flow equation for p_0 and then solving the mechanics equation for getting $\mathbf{u}_0$.

3 Iterative solvers

In this section, we present several monolithic and splitting iterative solvers for Eq. 4. First, we propose the Newton method which is well known for having locally quadratic convergence. Secondly, we combine the Newton method with a stabilized splitting method similar to the undrained splitting method. Finally, for the third and fourth solvers, we propose monolithic and splitting L-schemes. The L-scheme can be interpreted as either a stabilized Picard method or a quasi-Newton method. This scheme is robust but only linearly convergent. Moreover, it can be applied to non-smooth but monotonically increasing non-linearities. For example, for the case of Hölder continuous (not Lipschitz) non-linearities we refer to [13]. As it is a fixed point scheme, it can be speeded up by using the Anderson acceleration [2, 15]. To summarize, the main advantages of the L-scheme are:

- It does not involve computation of derivatives.
- The arising linear systems are well-conditioned.

– It can be applied to non-smooth nonlinearities.
– It is easy to understand and implement.

The iterative solvers will be written using an incremental formulation. In this regard, we introduce naturally defined residuals for the non-linear Eq. 4.

$$\begin{aligned}\mathcal{F}_{mech}(\mathbf{u},\, p) &= -\nabla\cdot\boldsymbol{\Pi}\,(\nabla\mathbf{u},\, p) - \rho_b\mathbf{g},\\ \mathcal{F}_{darcy}(\mathbf{u},\, p) &= \mathbf{q} + \mathbf{K}(\nabla\mathbf{u})\left(\nabla p - \rho_{f,ref}\mathbf{G}(\nabla\mathbf{u})\right),\\ \mathcal{F}_{mass}(\mathbf{u},\, p) &= \dot{\Gamma}(\mathbf{u},\, p) + \nabla\cdot\mathbf{q} - S_f.\end{aligned} \tag{5}$$

We will denote by $\delta(\cdot)^i = (\cdot)^i - (\cdot)^{i-1}$ the incremental operator, i the incremental counter, $\partial_{(\cdot)}$ the partial derivative operator with respect to $(\cdot)$.

3.1 A monolithic Newton

The Newton method is usually the first choice of the linearization methods due to its quadratic convergence. However, the convergence is local and it requires relatively small time steps to ensure the quadratic convergence [46]. The method starts by using initial solution $\left(\mathbf{u}^0, \mathbf{q}^0, p^0\right)$, solves for $\left(\delta\mathbf{u}^i, \delta\mathbf{q}^i, \delta p^i\right)$ satisfying:

$$\begin{aligned}&-\nabla\cdot\left(\partial_{\mathbf{u}}\boldsymbol{\Pi}\left(\nabla\mathbf{u}^{i-1}, p^{i-1}\right)\nabla\delta\mathbf{u}^i - \partial_p\boldsymbol{\Pi}\left(\nabla\mathbf{u}^{i-1}, p^{i-1}\right)\delta p^i\right)\\ &\quad= -\mathcal{F}_{mech}(\mathbf{u}^{i-1}, p^{i-1}),\\ &\delta\mathbf{q}^i + \partial_{\mathbf{u}}\left(\mathbf{K}(\nabla\mathbf{u}^{i-1})\left(\nabla p^{i-1} - \rho_{f,ref}\mathbf{G}(\nabla\mathbf{u}^{i-1})\right)\right)\delta\mathbf{u}^i\\ &\quad+\mathbf{K}(\nabla\mathbf{u}^{i-1})\nabla\delta p^{i-1} = -\mathcal{F}_{darcy}(\mathbf{u}^{i-1}, p^{i-1}),\\ &\partial_p\dot{\Gamma}(\mathbf{u}^{i-1}, p^{i-1})\delta p^i + \partial_{\mathbf{u}}\dot{\Gamma}(\mathbf{u}^{i-1}, p^{i-1})\delta\mathbf{u}^i + \nabla\cdot\delta\mathbf{q}^i\\ &\quad= -\mathcal{F}_{mass}(\mathbf{u}^{i-1}, p^{i-1}),\end{aligned} \tag{6}$$

and finally updates the variables:

$$\left(\mathbf{u}^i, \mathbf{q}^i, p^i\right) = \left(\mathbf{u}^{i-1}, \mathbf{q}^{i-1}, p^{i-1}\right) + \left(\delta\mathbf{u}^i, \delta\mathbf{q}^i, \delta p^i\right).$$

Where $\partial_{\mathbf{u}}\boldsymbol{\Pi}$ is a fourth-order tensor representing the partial gradient of $\boldsymbol{\Pi}$ with respect $\mathbf{u}$.

3.2 An alternate Newton

The alternate Newton method combines a splitting method with the Newton linearization. We introduce a stabilization parameter $L_s \geq 0$ to stabilize the mechanics equation. Thus resembling the undrained splitting scheme, even though the iterative steps start with the flow problem first as in the fixed stress method. The precise condition on L_s to ensure convergence is shown in Theorem 2. The method consists of two steps: starting with the initial condition $\left(\mathbf{u}^0, \mathbf{q}^0, p^0\right)$:

Step 1: Solve for $\left(\delta\mathbf{q}^i, \delta p^i\right)$

$$\begin{aligned}\delta\mathbf{q}^i + \mathbf{K}(\nabla\mathbf{u}^{i-1})\nabla\delta p^{i-1} &= -\mathcal{F}_{darcy}(\mathbf{u}^{i-1}, p^{i-1}),\\ \partial_p\dot{\Gamma}(\mathbf{u}^{i-1}, p^{i-1})\delta p^i + \nabla\cdot\delta\mathbf{q}^i &= -\mathcal{F}_{mass}(\mathbf{u}^{i-1}, p^{i-1}),\end{aligned} \tag{7}$$

and update the variables

$$\left(\mathbf{q}^i, p^i\right) = \left(\mathbf{q}^{i-1}, p^{i-1}\right) + \left(\delta\mathbf{q}^i, \delta p^i\right).$$

Step 2: Solve for $\delta\mathbf{u}^i$ satisfying

$$\begin{aligned}&-\nabla\cdot\left(\partial_{\mathbf{u}}\boldsymbol{\Pi}\left(\nabla\mathbf{u}^{i-1}, p^i\right)\nabla\delta\mathbf{u}^i - L_s(\nabla\cdot\delta\mathbf{u}^i)\,\mathbf{I}\right)\\ &\quad= -\mathcal{F}_{mech}(\mathbf{u}^{i-1}, p^i),\end{aligned} \tag{8}$$

and update the variable

$$\mathbf{u}^i = \mathbf{u}^{i-1} + \delta\mathbf{u}^i.$$

3.3 A monolithic *L*-scheme

A monolithic L-scheme requires three constant tensors $\mathbf{L_u},\ \mathbf{L}_p,\ \mathbf{L_q} \in \mathbb{R}^{d\times d}$ and two positive constants L_p and $L_{\mathbf{u}}$ as linearization parameters. A practical choice of the linearization parameters will be discussed in the numerical section. We refer to [11, 23] for a discussion regarding the best choice for the linearization parameters L_p and $L_{\mathbf{u}}$.

The method starts with the given initial solution $\left(\mathbf{u}^0, \mathbf{q}^0, p^0\right)$ and solve for $\left(\delta\mathbf{u}^i, \delta\mathbf{q}^i, \delta p^i\right)$:

$$\begin{aligned}-\nabla\cdot\mathbf{L_u}\nabla\delta\mathbf{u}^i - \nabla\cdot\mathbf{L}_p\delta p^i &= -\mathcal{F}_{mech}(\mathbf{u}^{i-1}, p^{i-1}),\\ \delta\mathbf{q}^i + \mathbf{K}(\nabla\mathbf{u}^{i-1})\nabla\delta p^i + \mathbf{L_q}\delta\mathbf{u}^i &= -\mathcal{F}_{darcy}(\mathbf{u}^{i-1}, p^{i-1}),\\ L_p\delta p^i + L_{\mathbf{u}}\delta\mathbf{u}^i + \nabla\cdot\delta\mathbf{q}^i &= -\mathcal{F}_{mass}(\mathbf{u}^{i-1}, p^{i-1}),\end{aligned} \tag{9}$$

and then update the variables

$$\left(\mathbf{u}^i, \mathbf{q}^i, p^i\right) = \left(\mathbf{u}^{i-1}, \mathbf{q}^{i-1}, p^{i-1}\right) + \left(\delta\mathbf{u}^i, \delta\mathbf{q}^i, \delta p^i\right).$$

3.4 A splitting *L*-scheme

The splitting scheme requires fewer linearization terms: two constants $\mathbf{L_u} \in \mathbb{R}^{d\times d}$, $L_p \geq 0$ and a positive stabilization term L_s. This makes it suitable for quick implementation since there is no need to calculate any Jacobian. The method is split in two steps, given initial solution $\left(\mathbf{u}^0, \mathbf{q}^0, p^0\right)$:

Step 1: Solve for $\left(\delta\mathbf{q}^i, \delta p^i\right)$

$$\begin{aligned}\delta\mathbf{q}^i + \mathbf{K}(\nabla\mathbf{u}^{i-1})\nabla\delta p^i &= -\mathcal{F}_{darcy}(\mathbf{u}^{i-1}, p^{i-1}),\\ L_p\delta p^i + \nabla\cdot\delta\mathbf{q}^i &= -\mathcal{F}_{mass}(\mathbf{u}^{i-1}, p^{i-1}),\end{aligned} \tag{10}$$

update the variables

$$\left(\mathbf{q}^i, p^i\right) = \left(\mathbf{q}^{i-1}, p^{i-1}\right) + \left(\delta\mathbf{q}^i, \delta p^i\right).$$

Step 2: Solve for $\delta \mathbf{u}^i$

$$-\nabla \cdot \left(\mathbf{L}_{\mathbf{u}} \nabla \delta \mathbf{u}^i + L_s (\nabla \delta \cdot \mathbf{u}^i)\, \mathbf{I} \right) = -\mathcal{F}_{mech}(\mathbf{u}^{i-1}, p^i), \quad (11)$$

and then update the variables

$$\mathbf{u}^i = \mathbf{u}^{i-1} + \delta \mathbf{u}^i.$$

4 The Biot model under small deformations

The convergence analysis of the iterative solvers proposed cannot be addressed with standard techniques [11, 14, 15, 37, 39]. This is due to the non-linearities being non-monotone. Nevertheless, a rigorous analysis can be performed for the case of small deformations. Accordingly, we assume the porous medium to be under small deformation and present the convergence of the iterative solvers proposed in the previous section.

Under small deformation, the difference between Ω_t and Ω can be neglected. The gradient of the transformation is approximated by $\mathbf{F} \approx \mathbf{I}$ and the determinant of the transformation by $J \approx 1$. Additionally, the Green strain tensor $\mathbf{E}$ can be approximated by the infinitesimal strain tensor $\mathbf{E} \approx \varepsilon = \frac{1}{2}\left(\nabla \mathbf{u} + (\nabla \mathbf{u})^\top\right)$. Then, the poroelastic stress tensor can be expressed by:

$$\mathbf{\Pi}(\mathbf{u}, p) = \sigma(\mathbf{u}, p) = 2\mu\varepsilon(\nabla \mathbf{u}) + \mathfrak{c}(\mathrm{tr}(\varepsilon(\nabla \mathbf{u})))\mathbf{I} - \alpha p \mathbf{I}, \quad (12)$$

where α is the Biot constant. The mobility tensor is considered isotropic $\mathbf{K}(\mathbf{u}, p) = k\mathbf{I}$, but the results of the convergence analysis can be extended without difficulties to a more general anisotropic case. Additionally, the time derivative of the volumetric deformation is approximated by $\dot{J} \approx \nabla \cdot \dot{\mathbf{u}}$. In this regard, the fluid mass can be expressed as:

$$\dot{\Gamma}(\mathbf{u}, p) = \dot{\mathfrak{b}}(p) + \alpha \nabla \cdot \dot{\mathbf{u}}, \quad (13)$$

where the relative density $\mathfrak{b}(\cdot)$ is a non-linear function of the pressure p. The variational formulation for the Biot model, under small deformation, reads as follows:

For each $t \in (0, T]$, find $\mathbf{u}(t) \in \left(H_0^1(\Omega)\right)^d$, $\mathbf{q} \in H(\mathrm{div}, \Omega)$, and $p(t) \in L^2(\Omega)$ such that there holds:

$$\begin{aligned}
(\varepsilon(\mathbf{u}), \varepsilon(\mathbf{v})) + (\mathfrak{c}(\nabla \cdot \mathbf{u}) - \alpha p, \nabla \cdot \mathbf{v}) &= (\rho_b \mathbf{g}, \mathbf{v}), \quad \forall \mathbf{v} \in (H(\Omega))^d, \\
\left(\mathbf{K}^{-1}\mathbf{q}, \mathbf{z}\right) - (p, \nabla \cdot \mathbf{z}) &= \left(\rho_f \mathbf{g}, \mathbf{z}\right), \quad \forall \mathbf{z} \in H(\mathrm{div}, \Omega), \\
\left(\dot{\mathfrak{b}}(p) + \alpha \nabla \cdot \dot{\mathbf{u}}, w\right) + (\nabla \cdot \mathbf{q}, w) &= \left(S_f, w\right), \quad \forall w \in L^2(\Omega), \quad (14)
\end{aligned}$$

with the initial condition:

$$(\mathfrak{b}(p_0) + \alpha \nabla \cdot \mathbf{u}_0, w) = 0, \ \forall w \in L^2(\Omega). \quad (15)$$

In the above, we have used the standard notations. We denote by $L^2(\Omega)$ the space of square integrable functions and by $H^1(\Omega)$ the Sobolev space $H^1(\Omega) = \{v \in L^2(\Omega)\,;\ \nabla v \in L^2(\Omega)^d\}$. Furthermore, $H_0^1(\Omega)$ is the space of functions in $H^1(\Omega)$ vanishing on $\partial\Omega$ and $H(\mathrm{div}; \Omega)$ the space of vector valued function having all the components and the divergence in $L^2(\Omega)$. As usual, we denote by $(\cdot, \cdot)$ the inner product in $L^2(\Omega)$, and by $||\cdot||$ its associated norm.

Next, we make structural assumptions on the non-linearities:

(A1) $\mathfrak{c}, \mathfrak{b} : \mathbb{R} \to \mathbb{R}$ differentiable with $\mathfrak{c}'$ and $\mathfrak{b}'$ Lipschitz continuous.

(A2) There exists a constant $\alpha_{\mathfrak{c}}$ such that $\mathfrak{c}'(\xi) > \alpha_{\mathfrak{c}}$, $\forall \xi \in \mathbb{R}$.

(A3) There exists a constant $\alpha_{\mathfrak{b}}$ such that $\mathfrak{b}'(\xi) > \alpha_{\mathfrak{b}}$, $\forall \xi \in \mathbb{R}$.

(A4) There exists constant $k_m > 0$ and k_M such that $k_m \leq k(\boldsymbol{\xi}) \leq k_M$, $\forall \boldsymbol{\xi} \in \Omega$.

For the discretization of problem (14), we use continuous Galerkin finite elements for the displacement variable and mixed finite elements for the flow variables [24, 42]. More precisely, we use linear elements ($\mathbb{Q}_1^d$) for the displacement and lowest order Raviart-Thomas ($\mathbb{RT}$) for $d = 2$, or Raviart-Thomas-Nedelec ($\mathbb{RTN}$) for $d = 3$ [17], for the flow variables: flux and pressure. Backward Euler is used for the temporal discretization.

Let $\mathcal{K}_h$ be a regular decomposition of Ω into quadrilateral elements K for $d = 2$, and hexahedral elements for $d = 3$. We use quadrilateral and hexahedral elements because the implementation in deal.II is tailored to these [4]. We denote the diameter of the element K by h_K, and the global discretization mesh diameter by $h := \max_{K \in \mathcal{K}_h} h_K$. We introduce the finite element spaces $\mathbb{P}_p$ following the lines of Brezzi and Fortin [17] which are spaces of polynomials of degree p, for each component of the position vector $\mathbf{x}$. With that, we define the following vector-valued space:

$$\mathbb{Q}_p^d(K) := \begin{cases} \left\{\varphi : K \to \mathbb{R}^2 \,\middle|\, \varphi \in \mathbb{P}_p(K) \times \mathbb{P}_p(K)\right\}, & \text{if } d = 2 \\ \left\{\varphi : K \to \mathbb{R}^3 \,\middle|\, \varphi \in \mathbb{P}_p(K) \times \mathbb{P}_p(K) \times \mathbb{P}_p(K)\right\}, & \text{if } d = 3. \end{cases}$$

which is a space of vector-valued polynomials of degree p at each component. The continuous Galerkin (cG(1)) space is defined as:

$$\mathbf{V}_h := \left\{ \mathbf{v}_h \in C(\Omega) \,\middle|\, \mathbf{v}_{h|K} \in \mathbb{Q}_1^d(K), \forall K \in \mathcal{K}_h \right\}.$$

The mixed finite element (MFEM(0)) spaces are defined as:

$$\mathbf{Z}_h := \begin{cases} \left\{\mathbf{z}_h \in \mathbf{H}(\mathrm{div}; \Omega) \,\middle|\, \mathbf{z}_{h|K} \in \mathbb{RTN}_0(K), \forall K \in \mathcal{K}_h\right\}, & \text{if } d = 2 \\ \left\{\mathbf{z}_h \in \mathbf{H}(\mathrm{div}; \Omega) \,\middle|\, \mathbf{z}_{h|K} \in \mathbb{RTN}_0(K), \forall K \in \mathcal{K}_h\right\}, & \text{if } d = 3, \end{cases}$$

and

$$W_h := \begin{cases} \left\{w_h \in L^2(\Omega) \,\middle|\, w_{h|K} \in \mathbb{P}_0(K), \forall K \in \mathcal{K}_h\right\}, & \text{if } d = 2 \\ \left\{w_h \in L^2(\Omega) \,\middle|\, w_{h|K} \in \mathbb{P}_0(K), \forall K \in \mathcal{K}_h\right\}, & \text{if } d = 3. \end{cases}$$

The spaces cG(1) and MFEM(0) are not uniformly inf-sup stable for poromechanics problems. However, a small enough h can be used to avoid oscillations [50].

For $N \in \mathbb{N}$, we discretize the time interval uniformly and define the time step $\tau = \frac{T}{N}$ and $t_n = n\tau$. We use the index n for the primary variables $\mathbf{u}^n$, $\mathbf{q}^n$, and p^n at corresponding time step t_n. In this way, the fully discrete weak problem reads:

For $n \geq 1$ and given $\left(\mathbf{u}_h^{n-1}, \mathbf{q}_h^{n-1}, p_h^{n-1}\right)$ find $\left(\mathbf{u}_h^n, \mathbf{q}_h^n, p_h^n\right) \in (\mathbf{V}_h, \mathbf{Z}_h, W_h)$, such that:

$$
\begin{aligned}
\left(\varepsilon(\mathbf{u}_h^n), \varepsilon(\mathbf{v}_h)\right) + \left(\mathfrak{c}(\nabla \cdot \mathbf{u}_h^n), \nabla \cdot \mathbf{v}_h\right) - \left((\alpha p_h^n, \nabla \cdot \mathbf{v}_h\right) &= (\rho_b \mathbf{g}, \mathbf{v}_h), \\
\left(\mathbf{K}^{-1}\mathbf{q}_h^n, \mathbf{z}_h\right) - \left(p_h^n, \nabla \cdot \mathbf{z}_h\right) &= \left(\rho_f \mathbf{g}, \mathbf{z}_h\right), \\
\left(\mathfrak{b}(p_h^n) - \mathfrak{b}(p_h^{n-1}), w_h\right) + \left(\alpha \nabla \cdot (\mathbf{u}_h^n - \mathbf{u}_h^{n-1}), w_h\right) & \\
+\tau\left(\nabla \cdot \mathbf{q}_h^n, w_h\right) &= \tau(S_f, w_h),
\end{aligned}
\tag{16}
$$

for all $(\mathbf{v}_h, \mathbf{z}_h, w_h) \in (\mathbf{V}_h, \mathbf{Z}_h, W_h)$.

Following the notation previously introduced, we denote by n the time level, whereas i will refer to the iteration number of the Newton method. We further denote the approximate solution of the linearized problem (16) by $(\mathbf{u}_h^{n,i}, \mathbf{q}_h^{n,i}, p_h^{n,i})$. At this stage, we can introduce the notations:

$$
\begin{aligned}
\mathbf{e}_{\mathbf{u}}^{n,i} &= \mathbf{u}_h^{n,i} - \mathbf{u}_h^n, \\
\mathbf{e}_{\mathbf{q}}^{n,i} &= \mathbf{q}_h^{n,i} - \mathbf{q}_h^n, \\
e_p^{n,i} &= p_h^{n,i} - p_h^n.
\end{aligned}
$$

These will be used subsequently in the convergence analysis of the monolithic Newton method and the alternate version. For the monolithic and splitting L-scheme, the convergence analysis can be found in [11].

4.1 Convergence analysis of the monolithic Newton solver

In this section, we analyze the monolithic Newton solver introduced in Section 3 used for solving the Biot model under small deformation given in Eq. 16. As we have previously stated, we perform the analysis for the case of small deformation. Here, we present a variational formulation of the scheme and demonstrate its quadratic convergence in a rigorous manner. The monolithic Newton solver reads as follows:

For $i = 1, 2, \ldots$ solve:

$$
\begin{aligned}
&\left(\varepsilon(\mathbf{u}_h^{n,i}), \varepsilon(\mathbf{v}_h)\right) + \left(\mathfrak{c}(\nabla \cdot \mathbf{u}_h^{n,i-1}) + \mathfrak{c}'(\nabla \cdot \mathbf{u}_h^{n,i-1})\nabla \cdot \delta\mathbf{u}_h^{n,i}, \nabla \cdot \mathbf{v}_h\right) \\
&- \left(\alpha p_h^{n,i}, \nabla \cdot \mathbf{v}_h\right) = (\rho_b \mathbf{g}, \mathbf{v}_h), \\
&\left(\mathbf{K}^{-1}\mathbf{q}_h^{n,i}, \mathbf{z}_h\right) - \left(p_h^{n,i}, \nabla \cdot \mathbf{z}_h\right) = \left(\rho_f \mathbf{g}, \mathbf{z}_h\right), \\
&\left(\mathfrak{b}(p_h^{n,i-1}) + \mathfrak{b}'(p_h^{n,i-1})\delta p_h^{n,i} - \mathfrak{b}(p_h^{n-1}), w_h\right) \\
&+ \left(\alpha \nabla \cdot (\mathbf{u}_h^{n,i} - \mathbf{u}_h^{n-1}), w_h\right) \\
&+\tau\left(\nabla \cdot \mathbf{q}_h^{n,i}, w_h\right) = \tau(S_f, w_h),
\end{aligned}
\tag{17}
$$

$\forall\, (\mathbf{v}_h, \mathbf{z}_h, w_h) \in (\mathbf{V}_h, \mathbf{Z}_h, W_h)$, where the initial approximation $(\mathbf{u}_h^{n,0}\mathbf{q}_h^{n,0}, p_h^{n,0})$ is taken as the solution at the previous time step, that is $(\mathbf{u}_h^{n-1}, \mathbf{q}_h^{n-1}, p_h^{n-1})$.

In order to prove the convergence of the monolithic Newton solver, the following lemma will be used.

Lemma 1 *If $f : \mathbb{R} \to \mathbb{R}$ is differentiable and f' is Lipschitz continuous, then there holds:*

$$
|f(x) - f(y) + f'(y)(y - x)| \leq \frac{L_{f'}}{2}|y - x|^2, \quad \forall\, x, y \in \mathbb{R},
$$

and $L_{f'}$ the Lipschitz costant of f'.

The proof can be found at p. 350 in [32], for example.

Next, the following result provides the quadratic convergence of the Newton method (17) for τ sufficiently small.

Theorem 1 *Assuming (A1)–(A4), the monolithic Newton solver in* Eq. 17 *converges quadratically if $\tau = O(h^{\frac{d}{2}})$.*

Proof By subtracting Eq. 16 from Eq. 17, taking as test functions $\mathbf{e}_{\mathbf{u}}^{n,i}$, $\mathbf{e}_{\mathbf{q}}^{n,i}$, and $e_p^{n,i}$ and rearranging some terms to the right-hand side we obtain:

$$
\begin{aligned}
&\left(\varepsilon(\mathbf{e}_{\mathbf{u}}^{n,i}), \varepsilon(\mathbf{e}_{\mathbf{u}}^{n,i})\right) + \left(\mathfrak{c}'(\nabla \cdot \mathbf{u}_h^{n,i-1})\nabla \cdot \mathbf{e}_{\mathbf{u}}^{n,i}, \nabla \cdot \mathbf{e}_{\mathbf{u}}^{n,i}\right) \\
&- \left(\alpha e_p^{n,i}, \nabla \cdot \mathbf{e}_{\mathbf{u}}^{n,i}\right) \\
&= \left(\mathfrak{c}(\nabla \cdot \mathbf{u}_h^n) - \mathfrak{c}(\nabla \cdot \mathbf{u}_h^{n,i-1}) + \mathfrak{c}'(\nabla \cdot \mathbf{u}_h^{n,i-1})\nabla \right. \\
&\qquad \left. \cdot \mathbf{e}_{\mathbf{u}}^{n,i-1}, \nabla \cdot \mathbf{e}_{\mathbf{u}}^{n,i}\right),
\end{aligned}
\tag{18}
$$

$$
\left(\mathbf{K}^{-1}\mathbf{e}_{\mathbf{q}}^{n,i}, \mathbf{e}_{\mathbf{q}}^{n,i}\right) - \left(e_p^{n,i}, \nabla \cdot \mathbf{e}_{\mathbf{q}}^{n,i}\right) = 0, \tag{19}
$$

$$
\begin{aligned}
&\left(\mathfrak{b}'(p_h^{n,i-1})\left(p_h^{n,i} - p_h^n\right), e_p^{n,i}\right) + \left(\alpha \nabla \cdot \mathbf{e}_{\mathbf{u}}^{n,i}, e_p^{n,i}\right) \\
&+\tau\left(\nabla \cdot \mathbf{e}_{\mathbf{q}}^{n,i}, e_p^{n,i}\right) \\
&= \left(\mathfrak{b}(p_h^{n,i-1}) - \mathfrak{b}(p_h^{n-1}) + \mathfrak{b}'(p_h^{n,i-1})\left(p_h^{n,i-1} - p_h^n\right), e_p^{n,i}\right),
\end{aligned}
\tag{20}
$$

where we have rewritten:

$$\begin{aligned}\mathfrak{c}'(\nabla\cdot\mathbf{u}_h^{n,i-1})\nabla\cdot\delta\mathbf{u}_h^{n,i} &= \mathfrak{c}'(\nabla\cdot\mathbf{u}_h^{n,i-1})\nabla\cdot(\mathbf{u}_h^{n,i}-\mathbf{u}_h^{n,i-1})\\ &= \mathfrak{c}'(\nabla\cdot\mathbf{u}_h^{n,i-1})(\nabla\cdot\mathbf{u}_h^{n,i}-\nabla\cdot\mathbf{u}_h^{n})\\ &\quad -\mathfrak{c}'(\nabla\cdot\mathbf{u}_h^{n,i-1})(\nabla\cdot\mathbf{u}_h^{n,i-1}-\nabla\cdot\mathbf{u}_h^{n})\\ &= \mathfrak{c}'(\nabla\cdot\mathbf{u}_h^{n,i-1})\left(\nabla\cdot\mathbf{e}_{\mathbf{u}}^{n,i}-\nabla\cdot\mathbf{e}_{\mathbf{u}}^{n,i-1}\right),\end{aligned}$$

We obtain an analogous expression for the term with $\mathfrak{b}'(\cdot)$. From (A1), $\mathfrak{c}(\cdot)$ is differentiable with $\mathfrak{c}'(\cdot)$ Lipschitz continuous, then from Lemma 1 we have:

$$|\mathfrak{c}(x)-\mathfrak{c}(y)+\mathfrak{c}'(y)(y-x)|\leq\frac{L_{\mathfrak{c}'}}{2}|x-y|^2,\quad\forall x,y\in\mathbb{R},\tag{21}$$

where $L_{\mathfrak{c}'}$ represents the Lipschitz constant of $\mathfrak{c}'(\cdot)$. Then, by using Young's inequality $(a,b)\leq\frac{||a||^2}{2\gamma}+\frac{\gamma||b||^2}{2}$, for $\gamma\geq 0$, and by choosing $x=\nabla\cdot\mathbf{u}_h^n$ and $y=\nabla\cdot\mathbf{u}_h^{n,i-1}$ in Eq. 21, from Eq. 18 we obtain the following bound, for any $\gamma\geq 0$:

$$\begin{aligned}&||\varepsilon(\mathbf{e}_{\mathbf{u}}^{n,i})||^2+\left(\mathfrak{c}'(\nabla\cdot\mathbf{u}_h^{n,i-1})\nabla\cdot\mathbf{e}_{\mathbf{u}}^{n,i},\nabla\cdot\mathbf{e}_{\mathbf{u}}^{n,i}\right)-\left(\alpha e_p^{n,i},\nabla\cdot\mathbf{e}_{\mathbf{u}}^{n,i}\right)\\ &\leq\frac{L_{\mathfrak{c}'}^2}{8\gamma}||\nabla\cdot\mathbf{e}_{\mathbf{u}}^{n,i-1}||^4_{L^4(\Omega)}+\frac{\gamma}{2}||\nabla\cdot\mathbf{e}_{\mathbf{u}}^{n,i}||^2.\end{aligned}\tag{22}$$

Next, by using the inverse inequality for discrete spaces $||\cdot||_{L^4(\Omega)}\leq Ch^{-d/4}||\cdot||$ [16], (p. 111) the latter reads:

$$\begin{aligned}&||\varepsilon(\mathbf{e}_{\mathbf{u}}^{n,i})||^2+\left(\mathfrak{c}'(\nabla\cdot\mathbf{u}_h^{n,i-1})\nabla\cdot\mathbf{e}_{\mathbf{u}}^{n,i},\nabla\cdot\mathbf{e}_{\mathbf{u}}^{n,i}\right)-\left(\alpha e_p^{n,i},\nabla\cdot\mathbf{e}_{\mathbf{u}}^{n,i}\right)\\ &\leq C_1h^{-d}\frac{L_{\mathfrak{c}'}^2}{8\gamma}||\nabla\cdot\mathbf{e}_{\mathbf{u}}^{n,i-1}||^4+\frac{\gamma}{2}||\nabla\cdot\mathbf{e}_{\mathbf{u}}^{n,i}||^2.\end{aligned}\tag{23}$$

Finally, by using (A2) and choosing $\gamma=\alpha_{\mathfrak{c}}$, we obtain the following inequality:

$$\begin{aligned}||\varepsilon(\mathbf{e}_{\mathbf{u}}^{n,i})||^2\ &+\frac{\alpha_{\mathfrak{c}}}{2}||\nabla\cdot\mathbf{e}_{\mathbf{u}}^{n,i}||^2-\left(\alpha e_p^{n,i},\nabla\cdot\mathbf{e}_{\mathbf{u}}^{n,i}\right)\\ &\leq C_1h^{-d}\frac{L_{\mathfrak{c}'}^2}{8\alpha_{\mathfrak{c}}}||\nabla\cdot\mathbf{e}_{\mathbf{u}}^{n,i-1}||^4.\end{aligned}\tag{24}$$

In a similar way, we obtain the following expression from Eq. 20:

$$\begin{aligned}\tau\left(\nabla\cdot\mathbf{e}_{\mathbf{q}}^{n,i},e_p^{n,i}\right)\ &+\frac{\alpha_{\mathfrak{b}}}{2}||e_p^{n,i}||^2+\left(\alpha\nabla\cdot\mathbf{e}_{\mathbf{u}}^{n,i},e_p^{n,i}\right)\\ &\leq C_2h^{-d}\frac{L_{\mathfrak{b}'}^2}{8\alpha_{\mathfrak{b}}}||e_p^{n,i-1}||^4.\end{aligned}\tag{25}$$

Adding Eqs. 24, 25, and 19 multiplied by τ yields:

$$\begin{aligned}&||\varepsilon(\mathbf{e}_{\mathbf{u}}^{n,i})||^2+\frac{\alpha_{\mathfrak{c}}}{2}||\nabla\cdot\mathbf{e}_{\mathbf{u}}^{n,i}||^2+\frac{\alpha_{\mathfrak{b}}}{2}||e_p^{n,i}||^2+\tau\left(\mathbf{K}^{-1}\mathbf{e}_{\mathbf{q}}^{n,i},\mathbf{e}_{\mathbf{q}}^{n,i}\right)\\ &\leq C_1h^{-d}\frac{L_{\mathfrak{c}'}^2}{8\alpha_{\mathfrak{c}}}||\nabla\cdot\mathbf{e}_{\mathbf{u}}^{n,i-1}||^4+C_2h^{-d}\frac{L_{\mathfrak{b}'}^2}{8\alpha_{\mathfrak{b}}}||e_p^{n,i-1}||^4.\end{aligned}\tag{26}$$

By defining $\alpha_{\mathfrak{c},\mathfrak{b}}=\min\left(1,\alpha_{\mathfrak{c}},\alpha_{\mathfrak{b}},\frac{\tau}{k_M}\right)$ and $C_{\mathfrak{c},\mathfrak{b}}=\max\left(\frac{C_1L_{\mathfrak{c}'}^2}{\alpha_{\mathfrak{c}}},\frac{C_2L_{\mathfrak{b}'}^2}{\alpha_{\mathfrak{b}}}\right)$, we can rewrite Eq. 26 as:

$$\|\nabla\cdot\mathbf{e}_{\mathbf{u}}^{n,i}\|^2+\|e_p^{n,i}\|^2\leq\frac{C_{\mathfrak{c},\mathfrak{b}}h^{-d}}{\alpha_{\mathfrak{c},\mathfrak{b}}}\left(\|\nabla\cdot\mathbf{e}_{\mathbf{u}}^{n,i-1}\|^4+\|e_p^{n,i-1}\|^4\right).\tag{27}$$

Using $\|\nabla\cdot\mathbf{e}_{\mathbf{u}}^{n,0}\|\leq C\tau$, $\|e_p^{n,0}\|\leq C\tau$ (which can be proven), the quadratic convergence of Newton's method is ensured if:

$$\frac{C_{\mathfrak{c},\mathfrak{b}}h^{-d}}{\alpha_{\mathfrak{c},\mathfrak{b}}}\tau^2\leq 1$$

which holds true for $\tau^2h^{-d}=O(1)$, i.e. $\tau=O(h^{\frac{d}{2}})$. □

4.2 Convergence analysis of the alternate Newton solver

In this section, we present the splitting Newton solver for solving the non-linear Biot model given in Eq. 16. We present the solver in a variational form and demonstrate its linear convergence.

Let $i\geq 1$, $L_s\geq 0$ and $(\mathbf{u}_h^{n,i-1},\mathbf{q}_h^{n,i-1},p_h^{n,i-1})\in(\mathbf{V}_h,\mathbf{Z}_h,W_h)$ be given.

Step 1: Find $(\mathbf{q}_h^{n,i},p_h^{n,i})\in(\mathbf{Z}_h,W_h)$ such that:

$$\begin{aligned}&\left(\mathbf{K}^{-1}\mathbf{q}_h^{n,i},\mathbf{z}_h\right)-\left(p_h^{n,i},\nabla\cdot\mathbf{z}_h\right)=\left(\rho_f\mathbf{g},\mathbf{z}_h\right),\\ &\left(\mathfrak{b}(p_h^{n,i-1})+\mathfrak{b}'(p_h^{n,i-1})\delta p_h^{n,i}-\mathfrak{b}(p_h^{n-1}),w_h\right)\\ &+\tau\left(\nabla\cdot\mathbf{q}_h^{n,i},\nabla w_h\right)\\ &+\left(\alpha\nabla\cdot(\mathbf{u}_h^{n,i-1}-\mathbf{u}_h^{n-1}),w_h\right)=\tau(S_f,w_h),\end{aligned}\tag{28}$$

$\forall(\mathbf{z}_h,w_h)\in(\mathbf{Z}_h,W_h)$

Step 2: Find $\mathbf{u}_h^{n,i}\in\mathbf{V}_h$ such that:

$$\begin{aligned}&\left(\varepsilon(\mathbf{u}_h^{n,i}),\varepsilon(\mathbf{v}_h)\right)+\left(\mathfrak{c}(\nabla\cdot\mathbf{u}_h^{n,i-1})+\mathfrak{c}'(\nabla\cdot\mathbf{u}_h^{n,i-1})\nabla\right.\\ &\left.\cdot\delta\mathbf{u}_h^{n,i},\nabla\cdot\mathbf{v}_h\right)\\ &+\left(L_s\nabla\cdot\delta\mathbf{u}_h^{n,i},\nabla\cdot\mathbf{v}_h\right)-\left(\alpha p_h^{n,i},\nabla\cdot\mathbf{v}_h\right)=(\rho_b\mathbf{g},\mathbf{v}_h),\end{aligned}\tag{29}$$

$\forall\mathbf{v}_h\in\mathbf{V}_h$.

Table 2 Test cases with different non-linear compressibility $\mathfrak{b}(\cdot)$ and non-linear volumetric strain for $\mathfrak{c}(\cdot)$

Case	$\mathfrak{b}(p)$	$\mathfrak{c}(\nabla \cdot \mathbf{u})$
1	e^p	$(\nabla \cdot \mathbf{u})^3 + \nabla \cdot \mathbf{u}$
2	e^p	$(\nabla \cdot \mathbf{u})^3$
3	e^p	$\sqrt[3]{(\nabla \cdot \mathbf{u})^5} + \nabla \cdot \mathbf{u}$
4	p^2	$\nabla \cdot \mathbf{u}^2$

Theorem 2 *Assuming (A1)–(A4) and* $L_s \geq \frac{\alpha^2}{\alpha_{\mathfrak{b}}}$, *the alternate Newton solver in* Eqs. 28–29 *converges linearly if* τ *is small enough.*

Proof The proof is similar to that of Theorem 1. Nevertheless, for the sake of completion, we give it in Appendix A. □

5 Numerical examples

In this section, we present numerical experiments that illustrate the performance of the proposed iterative solvers. We study two test problems: a 2D academic problem with a manufactured analytical solution, and a 3D large deformation case on a unit cube. All numerical experiments were implemented using the open-source finite element library Deal II [4]. For all numerical experiments, a Backward Euler scheme has been used for the time discretization. We consider continuous Galerkin cG(1) for $\mathbf{u}$ and lowest order of mixed finite element MFEM(0) for $\mathbf{q}$ and p. However, we would like to mention that any stable discretization can be considered instead. We define the iterative difference ε at iteration i as follows:

$$\varepsilon^i := \|p^i - p^{i-1}\| + \|\mathbf{q}^i - \mathbf{q}^{i-1}\| + \|\mathbf{u}^i - \mathbf{u}^{i-1}\|,$$

and as a stopping criterion for the solvers, we use $\varepsilon^i \leq 10^{-8}$. This stopping criterion is sufficient since the convergence results from Theorems 1 and 2 can also be obtained with this iterative difference [11].

Test problem 1: an academic example for Biot's model under small deformation

We solve the non-linear Biot problem under small deformation in the unit-square $\Omega = (0, 1)^2$ and until final time $T = 1$. This test case was proposed in [11] to study the

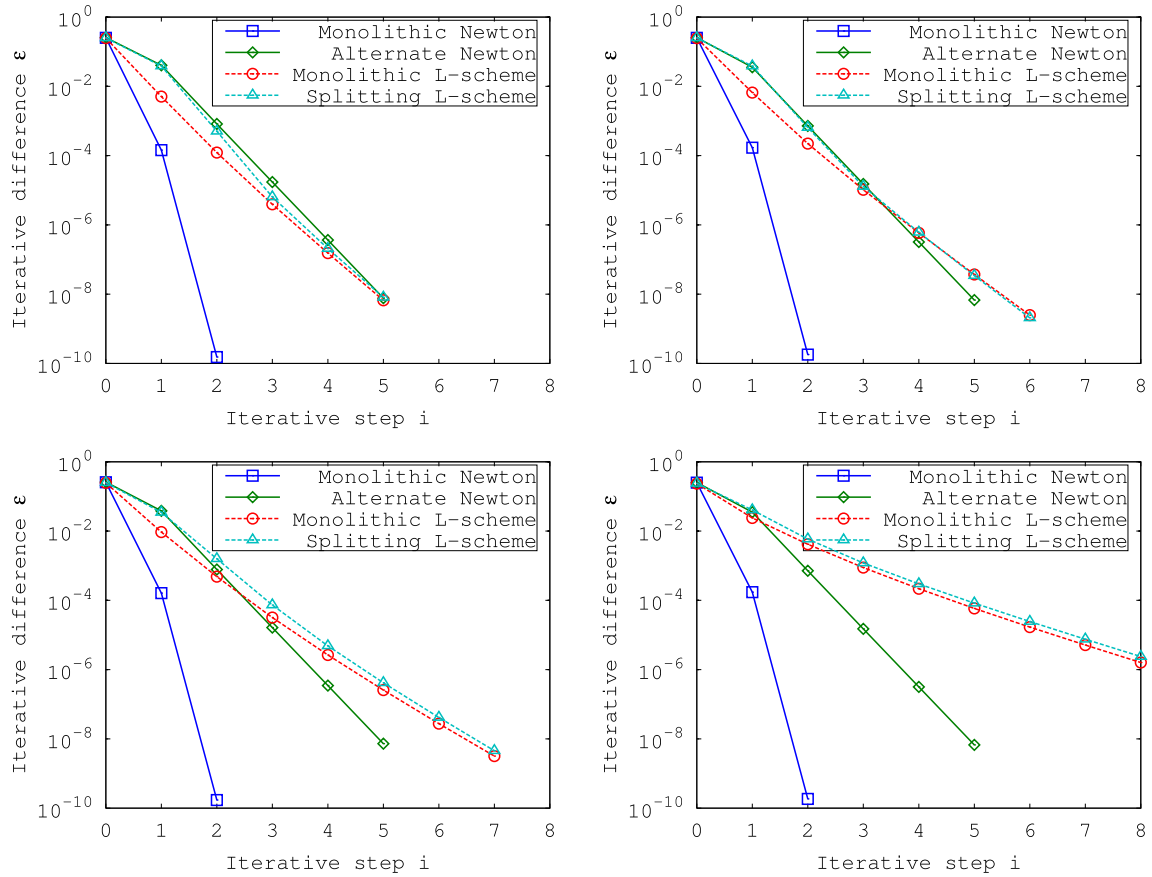

Fig. 1 Iterative difference ε^i at last time step $t = 1$: to the right $\mathfrak{b}(p) = e^p$, $\mathfrak{c}(\nabla \cdot \mathbf{u}) = \sqrt[3]{\mathbf{u}^5} + \nabla \cdot \mathbf{u}$, to the left $\mathfrak{b}(p) = p^2$, $\mathfrak{c}(\nabla \cdot \mathbf{u}) = (\nabla \cdot \mathbf{u})^2$

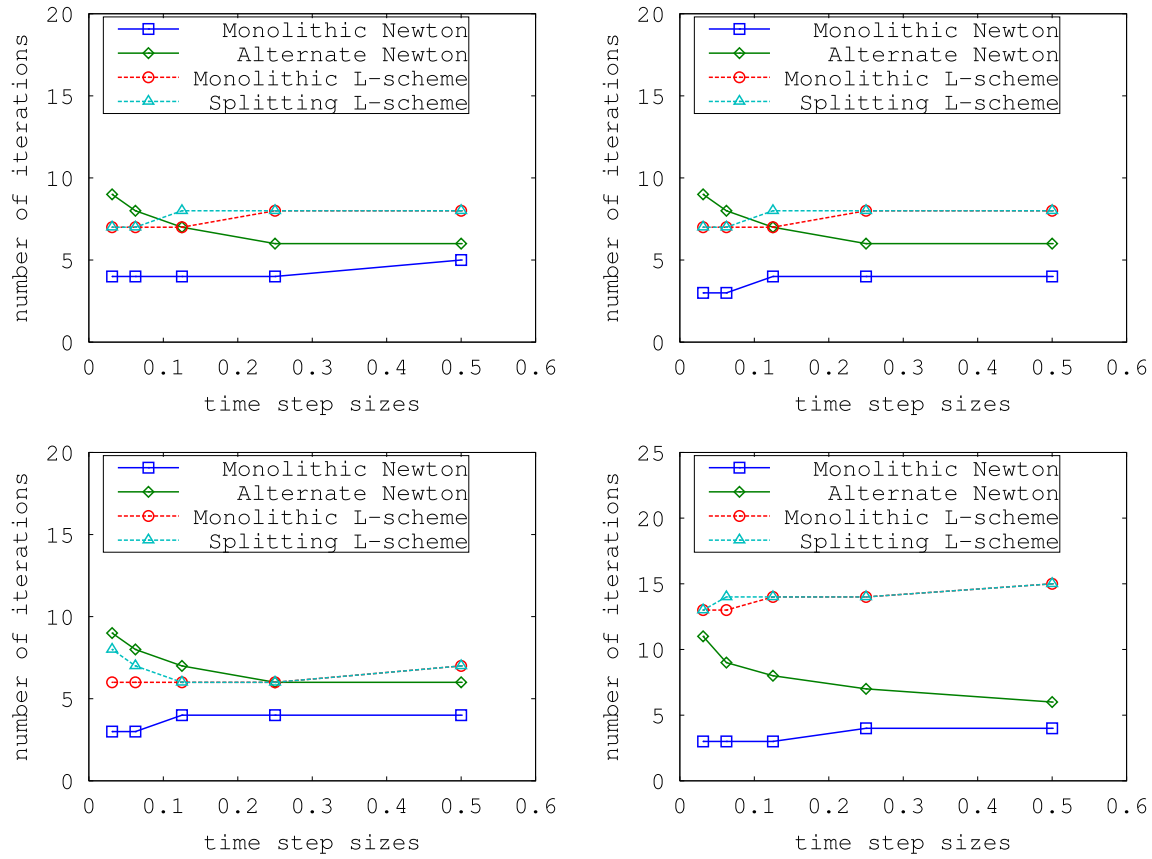

Fig. 2 Number of iteration for different time steps size at last time step $t = 1$: to the right $\mathfrak{b}(p) = e^p$, $\mathfrak{c}(\nabla \cdot \mathbf{u}) = \sqrt[3]{\mathbf{u}^5} + \nabla \cdot \mathbf{u}$, to the left $\mathfrak{b}(p) = p^2$, $\mathfrak{c}(\nabla \cdot \mathbf{u}) = (\nabla \cdot \mathbf{u})^2$

performance of the monolithic and splitting L-scheme. We extend the Newton method and the alternate Newton method described in Section 4.

Here, we use a manufactured right-hand side such that the problem admits the following analytical solution:

$$p(x, y, t) = tx(1-x)y(1-y), \quad \mathbf{q}(x, y, t) = -k\nabla p,$$
$$u_1(x, y, t) = u_2(x, y, t) = tx(1-x)y(1-y),$$

which it has homogeneous boundary values for p and $\mathbf{u}$.

For small deformations and vanishing rotations, there is no distinction between the reference and the deformed domains. In this regard, we solve problem (16) using the iterative solvers proposed in Section 4. The mesh size and the time step are set as $h = \tau = 0.1$. For this case, all initial conditions are zero. The linearization parameters L_p and $L_{\mathbf{u}}$ are equal to the Lipschitz constant $L_{\mathfrak{b}}$ and $L_{\mathfrak{c}}$ corresponding to the non-linearities $\mathfrak{b}(\cdot)$ and $\mathfrak{c}(\cdot)$ [11].

Table 3 Boundary conditions for Traction and Rotation case respectively

Face	Flow	Mechanics
Top	$p = 0$	$\mathbf{u} = (\mathbf{R}(\theta(t)) - \mathbf{I})\, X_0$
Bottom	$p = 0$	$\mathbf{u} \cdot \boldsymbol{n} = 0$
Lateral	$p = 0$	$\boldsymbol{\Pi} \cdot \boldsymbol{n} = 0$

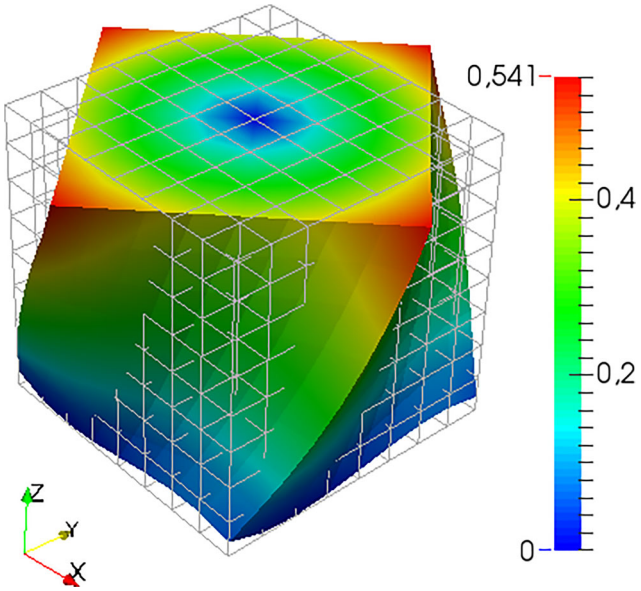

Fig. 3 Magnitude of the deformation field at final time $t = 1$ for test problem 2

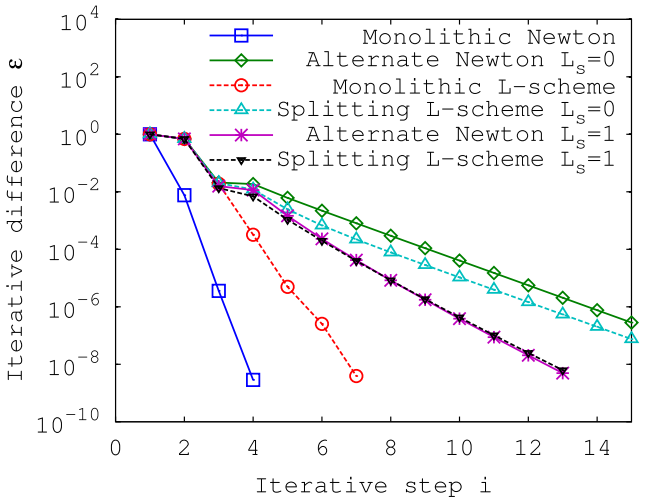

Fig. 4 Iterative difference ϵ^i at the last time step t=1 for test problem 2

In order to study the performance of the considered solvers, we propose in Table 2 several test cases with different non-linear compressibility $\mathfrak{b}(\cdot)$ and non-linear volumetric strain for $\mathfrak{c}(\cdot)$. Figure 1 shows the performance of the numerical methods at the last time step $T = 1$. The monolithic Newton method shows quadratic convergence in all cases. Nevertheless, the alternate Newton and the L-scheme methods show linear convergence as predicted in Section 4.

Figure 2 shows the performance of the considered solvers for different time steps. The Newton method has better convergence for smaller time steps while the L-scheme has it for larger time steps; all this is in agreement with the Theorems 1 and 2. The performance of the solvers are independent of the mesh discretization.

Test problem 2: a unit cube under large deformation

We now solve a large deformation problem on the unit cube $\Omega = (0, 1)^3$. A Lagrangian frame of reference is necessary to keep track of the deformed domain Ω_t at time t. We study the performance of the iterative solvers presented in Section 3 for solving Eq. 4. The material is supposed to be isotropic, with constant Lamé parameters μ and a non-linear volumetric strain $\mathfrak{c}(\cdot)$.

We will compare the iterative solvers for a torsion case on a unit cube. On the top face, we apply the rotation tensor $\mathbf{R}(\theta)$ of a time-dependent angle $\theta(t) = \pi/4\, t$, which gives a rotation of $\pi/4$ at $T = 1$. We set homogeneous initial condition for $(\mathbf{q}_0, p_0)$ and $\nabla \mathbf{u}_0 = (\mathbf{R}(\theta) - \mathbf{I})$. In the alternate Newton method, the stabilization parameter is set to $L_s = 1$. In the L-scheme method, the linearization tensor parameters are set as follows: $\mathbf{L_u} = \partial_{\mathbf{u}} \mathbf{\Pi}\,(\nabla \mathbf{u}_0, p_0)$, $\mathbf{L}_p = \partial_p \mathbf{\Pi}\,(\nabla \mathbf{u}_0, p_0)$, $\mathbf{L_q} = \partial_p \mathbf{K}\,(\nabla \mathbf{u}_0)$, $L_p = \partial_p \boldsymbol{\Gamma}\,(\nabla \mathbf{u}_0, p_0)$, and $L_{\mathbf{u}} = \partial_{\mathbf{u}} \boldsymbol{\Gamma}\,(\nabla \mathbf{u}_0, p_0)$. The mesh size and the time step are set as $h = \tau = 2^{-3}$. We denote by top face of the unit cube the region $z = 1$, the bottom face $z = 0$, and the lateral faces are $x = 0$, $x = 1$, $y = 0$, and $y = 1$. The boundary conditions are listed in Table 3 and the magnitude of the displacement field is shown in Fig. 3.

We compare the performance of the iterative solvers proposed in Section 3, and we observe that the numerical convergence is in accordance with the theory developed in Section 4, even though the analysis is done for small deformation. The monolithic Newton solver shows quadratic convergence and the alternate Newton solver shows linear convergence (see Fig. 4). None of these solvers is affected by the time step or mesh size. In contrast, the monolithic L-scheme shows a higher number of iteration for larger time steps (see Fig. 5). All splitting solvers have a slightly faster convergence when the stability term is used (we use $L_s = 1.0$).

6 Conclusions

We considered Biot's model under small and large deformations. Different solvers based on the L-scheme

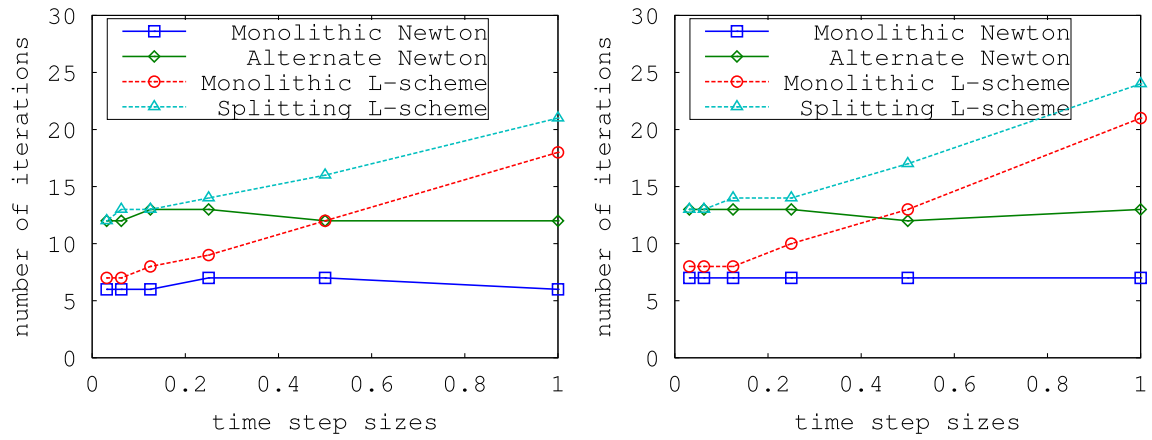

Fig. 5 Number of iterations at time $t = 1.0$ using different time step sizes: to the left $h = 1/2^3$, and $h = 1/2^4$ to the right

and Newton's method, in combination with monolithic and splitting schemes, were presented. The only quadratic convergent scheme is the monolithic Newton solver. The splitting Newton solver requires a stabilization parameter, otherwise the linear convergence cannot be guaranteed. The monolithic and alternate Newton solvers are robust with respect to the mesh size and time step size. The analysis of the solvers and illustrative numerical experiments were presented. We tested the performance of the solvers on two test problems: a unit square under small deformation and a unit cube under large deformation.

Acknowledgments The work was conducted as part of the Ph.D. thesis of Borregales Reverón M.A. at the University of Bergen. Nordbotten J.M. was funded in part by NRC grant number 250223. The research of Radu F.A. was partially supported by the VISTA project number AdaSim #6367. Kumar K. would like to acknowledge financial support from the project 811716 LAB2FIELD funded by the NRC. Open Access funding is provided by SINTEF AS.

Appendix A: Convergence proof of the alternate Newton method

The following result provides the linear convergence of the alternate Newton method in Eqs. 28 and 29 for τ sufficiently small. In order to prove convergence , the following lemmas will be used.

Lemma 2 *Let* $\{x_k\}_{k\geq 0}$ *be a sequence of real positive number satisfying:*

$$x_n \leq a x_{k-1}^2 + b x_{k-1} \ \forall n \geq 1, \tag{30}$$

where $a, b \geq 0$. *Assuming that*

$$a x_0^2 + b \leq 1$$

holds, then the sequence $\{x_k\}_{k\geq 0}$ *converges to zero.*

The result can be shown by induction; see p. 52 in [45] for more details.

Theorem 3 *Assuming (A1)–(A4) and* $L_s \geq \frac{\alpha^2}{\alpha_{\mathfrak{b}}}$, *the alternate Newton splitting method in* Eqs. 28 and 29 *converges linearly if* τ *is small enough.*

Proof By subtracting problems Eqs. 28 and 29 and 16, taking as test functions $\mathbf{e}_{\mathbf{q}}^{n,i}$, $e_p^{n,i}$, and $\mathbf{e}_{\mathbf{u}}^{n,i}$, and rearranging some elements to the right-hand side we obtain:

$$\left(\mathbf{K}^{-1}\mathbf{e}_{\mathbf{q}}^{n,i}, \mathbf{e}_{\mathbf{q}}^{n,i}\right) - \left(e_p^{n,i}, \nabla\cdot\mathbf{e}_{\mathbf{q}}^{n,i}\right) = 0, \tag{31}$$

$$\begin{aligned}&\left(\mathfrak{b}'(p_h^{n,i-1})(p_h^n - p_h^{n,i}), e_p^{n,i}\right) + \left(\alpha\nabla\cdot\mathbf{e}_{\mathbf{u}}^{n,i-1}, e_p^{n,i}\right) + \tau\left(\nabla\cdot\mathbf{e}_{\mathbf{q}}^{n,i}, e_p^{n,i}\right)\\ &= \left(\mathfrak{b}(p_h^n) - \mathfrak{b}(p_h^{n,i-1}) - \mathfrak{b}'(p_h^{n,i-1})(p_h^n - p_h^{n,i-1}), e_p^{n,i}\right).\end{aligned} \tag{32}$$

The mechanics equation then gives:

$$\begin{aligned}&\left(\varepsilon(\mathbf{e}_{\mathbf{u}}^{n,i}), \varepsilon(\mathbf{e}_{\mathbf{u}}^{n,i})\right) + \left(\mathfrak{c}'(\nabla\cdot\mathbf{u}_h^{n,i-1})\nabla\cdot\mathbf{e}_{\mathbf{u}}^{n,i}, \nabla\cdot\mathbf{e}_{\mathbf{u}}^{n,i}\right)\\ &+L_s\left(\nabla\cdot\delta\mathbf{u}_h^{n,i}, \nabla\cdot\mathbf{e}_{\mathbf{u}}^{n,i}\right) - \left(\alpha e_p^{n,i}, \nabla\cdot\mathbf{e}_{\mathbf{u}}^{n,i}\right)\\ &= \Big(\mathfrak{c}(\nabla\cdot\mathbf{u}_h^n) - \mathfrak{c}(\nabla\cdot\mathbf{u}_h^{n,i-1}) + \mathfrak{c}'(\nabla\cdot\mathbf{u}_h^{n,i-1})\nabla\\ &\cdot\mathbf{e}_{\mathbf{u}}^{n,i-1}, \nabla\cdot\mathbf{e}_{\mathbf{u}}^{n,i}\Big).\end{aligned} \tag{33}$$

By using similar steps as in Theorem 1, we obtain the following:

$$\begin{aligned}&||\varepsilon(\mathbf{e}_{\mathbf{u}}^{n,i})||^2 + \left(\mathfrak{c}'(\nabla\cdot\mathbf{u}_h^{n,i-1})\nabla\cdot\mathbf{e}_{\mathbf{u}}^{n,i}, \nabla\cdot\mathbf{e}_{\mathbf{u}}^{n,i}\right)\\ &+L_s\left(\nabla\cdot(\mathbf{e}_{\mathbf{u}}^{n,i} - \mathbf{e}_{\mathbf{u}}^{n,i-1}), \nabla\cdot\mathbf{e}_{\mathbf{u}}^{n,i}\right) - \left(\alpha e_p^{n,i}, \nabla\cdot\mathbf{e}_{\mathbf{u}}^{n,i}\right)\\ &\leq \frac{L_{\mathfrak{c}'}^2}{8\gamma_1}||\nabla\cdot\mathbf{e}_{\mathbf{u}}^{n,i-1}||_{L^4(\Omega)}^4 + \frac{\gamma_1}{2}||\nabla\cdot\mathbf{e}_{\mathbf{u}}^{n,i}||^2.\end{aligned} \tag{34}$$

Next, by using the inverse inequality $||\cdot||_{L^4(\Omega)} \leq Ch^{-d/4}||\cdot||$ [16], and by using the following formula $(x-y,x) = \frac{||x||^2}{2} + \frac{||x-y||^2}{2} - \frac{||y||^2}{2}$, by choosing $x = \nabla\cdot\mathbf{e_u}^{n,i}$ and $y = \nabla\cdot\mathbf{e}_{\mathbf{u}}^{n,i-1}$, we obtain from Eq. 34:

$$\begin{aligned}&||\varepsilon(\mathbf{e}_{\mathbf{u}}^{n,i})||^2 + \left(\mathfrak{c}'(\nabla\cdot\mathbf{u}_h^{n,i-1})\nabla\cdot\mathbf{e}_{\mathbf{u}}^{n,i}, \nabla\cdot\mathbf{e}_{\mathbf{u}}^{n,i}\right)\\ &+\frac{L_s}{2}||\nabla\cdot(\mathbf{e}_{\mathbf{u}}^{n,i} - \mathbf{e}_{\mathbf{u}}^{n,i-1})||^2\\ &\frac{L_s}{2}||\nabla\cdot\mathbf{e}_{\mathbf{u}}^{n,i}||^2 - \left(\alpha e_p^{n,i}, \nabla\cdot\mathbf{e}_{\mathbf{u}}^{n,i}\right) + \leq C_1 h^{-d}\frac{L_{\mathfrak{c}'}^2}{8\gamma_1}||\nabla\cdot\mathbf{e}_{\mathbf{u}}^{n,i-1}||^4\\ &+\frac{\gamma_1}{2}||\nabla\cdot\mathbf{e}_{\mathbf{u}}^{n,i}||^2 + \frac{L_s}{2}||\nabla\cdot\mathbf{e}_{\mathbf{u}}^{n,i-1}||^2.\end{aligned} \tag{35}$$

Finally, by reorganizing Eq. 35, using (A2) and choosing $\gamma_1 = \alpha_{\mathfrak{c}}$, we obtain the following inequality:

$$\begin{aligned}&||\varepsilon(\mathbf{e}_{\mathbf{u}}^{n,i})||^2 + \left(\frac{\alpha_{\mathfrak{c}} + L_s}{2}\right)||\nabla\cdot\mathbf{e}_{\mathbf{u}}^{n,i}||^2 + \frac{L_s}{2}||\nabla\cdot\delta\mathbf{e}_{\mathbf{u}}^{n,i}||^2\\ &\leq C_1 h^{-d}\frac{L_{\mathfrak{c}'}^2}{8\alpha_{\mathfrak{c}}}||\nabla\cdot\mathbf{e}_{\mathbf{u}}^{n,i-1}||^4 + \frac{L_s}{2}||\nabla\cdot\mathbf{e}_{\mathbf{u}}^{n,i-1}||\\ &+\left(\alpha e_p^{n,i}, \nabla\cdot\mathbf{e}_{\mathbf{u}}^{n,i}\right).\end{aligned} \tag{36}$$

In a similar way, we obtain the following expression from Eq. 20:

$$\frac{\tau}{k_M}||\mathbf{e}_{\mathbf{q}}^{n,i}||^2+\frac{\alpha_{\mathfrak{b}}}{2}||e_p^{n,i}||^2 \leq C_2 h^{-d}\frac{L_{\mathfrak{b}'}^2}{8\alpha_{\mathfrak{b}}}||e_p^{n,i-1}||^4-\alpha\left(\nabla\cdot\mathbf{e}_{\mathbf{u}}^{n,i-1}, e_p^{n,i}\right). \tag{37}$$

Adding Eqs. 36 and 37 yields:

$$\begin{aligned}&\frac{\tau}{k_M}||\mathbf{e}_{\mathbf{q}}^{n,i}||^2+\frac{\alpha_{\mathfrak{b}}}{2}||e_p^{n,i}||^2+||\varepsilon(\mathbf{e}_{\mathbf{u}}^{n,i})||^2+\frac{L_s}{2}||\nabla\cdot\delta\mathbf{e}_{\mathbf{u}}^{n,i}||^2\\&+\left(\frac{\alpha_{\mathfrak{c}}+L_s}{2}\right)||\nabla\cdot\mathbf{e}_{\mathbf{u}}^{n,i}||^2\\&\leq C_2 h^{-d}\frac{L_{\mathfrak{b}'}^2}{8\alpha_{\mathfrak{b}}}||e_p^{n,i-1}||^4+C_1 h^{-d}\frac{L_{\mathfrak{c}'}^2}{8\alpha_{\mathfrak{c}}}||\nabla\cdot\mathbf{e}_{\mathbf{u}}^{n,i-1}||^4\\&+\frac{L_s}{2}||\nabla\cdot\mathbf{e}_{\mathbf{u}}^{n,i-1}||^2+\left(\alpha\nabla\cdot\delta\mathbf{e}_{\mathbf{u}}^{n,i}, e_p^{n,i}\right).\end{aligned} \tag{38}$$

By using Young's inequality $(a,b) \leq \frac{||a||^2}{2\gamma}+\frac{\gamma||b||^2}{2}$, for $\gamma > 0$ and choosing $b = e_p^{n,i}$ and $a = \nabla\cdot\delta\mathbf{e}_{\mathbf{u}}^{n,i}$, we bound the coupling term (for $\gamma_2 > 0$):

$$\left(\alpha\nabla\cdot\delta\mathbf{e}_{\mathbf{u}}^{n,i}, e_p^{n,i}\right) \leq \frac{\alpha^2}{2\gamma_2}||\nabla\cdot\delta\mathbf{e}_{\mathbf{u}}^{n,i-1}||^2+\frac{\gamma_2}{2}||e_p^{n,i}||^2. \tag{39}$$

Then by using Eq. 39 and choosing $\gamma_2 = \frac{\alpha_{\mathfrak{b}}}{2}$, we obtain from Eq. 38:

$$\begin{aligned}&\frac{\tau}{k_M}||\mathbf{e}_{\mathbf{q}}^{n,i}||^2+\frac{\alpha_{\mathfrak{b}}}{4}||e_p^{n,i}||^2+||\varepsilon(\mathbf{e}_{\mathbf{u}}^{n,i})||^2+\left(\frac{L_s}{2}-\frac{\alpha^2}{2\alpha_{\mathfrak{b}}}\right)||\nabla\cdot\delta\mathbf{e}_{\mathbf{u}}^{n,i}||^2\\&+\left(\frac{\alpha_{\mathfrak{c}}+L_s}{2}\right)||\nabla\cdot\mathbf{e}_{\mathbf{u}}^{n,i}||^2 \leq \frac{h^{-d}}{8}\left(C_2\frac{L_{\mathfrak{b}'}^2}{\alpha_{\mathfrak{b}}}||e_p^{n,i-1}||^4\right.\\&\qquad\left.+C_1\frac{L_{\mathfrak{c}'}^2}{\alpha_{\mathfrak{c}}}||\nabla\cdot\mathbf{e}_{\mathbf{u}}^{n,i-1}||^4\right)\\&+\frac{L_s}{2}||\nabla\cdot\mathbf{e}_{\mathbf{u}}^{n,i-1}||^2.\end{aligned} \tag{40}$$

Since $L_s \geq \frac{\alpha^2}{\alpha_{\mathfrak{b}}}$, we obtain:

$$\begin{aligned}&\frac{\tau}{k_M}||\mathbf{e}_{\mathbf{q}}^{n,i}||^2+\frac{\alpha_{\mathfrak{b}}}{4}||e_p^{n,i}||^2+\left(\frac{\alpha_{\mathfrak{c}}+L_s}{2}\right)||\nabla\cdot\mathbf{e}_{\mathbf{u}}^{n,i}||^2\\&\leq \frac{h^{-d}}{8}\left(C_2\frac{L_{\mathfrak{b}'}^2}{\alpha_{\mathfrak{b}}}||e_p^{n,i-1}||^4+C_1\frac{L_{\mathfrak{c}'}^2}{\alpha_{\mathfrak{c}}}||\nabla\cdot\mathbf{e}_{\mathbf{u}}^{n,i-1}||^4\right)\\&\qquad+\frac{L_s}{2}||\nabla\cdot\mathbf{e}_{\mathbf{u}}^{n,i-1}||^2.\end{aligned} \tag{41}$$

By using $||\nabla\cdot\mathbf{e}_{\mathbf{u}}^{n,0}|| \leq C\tau$, $||e_p^{n,0}|| \leq C\tau$ which can be proven and the estimate in Lemma 2, the convergence is ensured if $\tau = O(h^{\frac{d}{2}})$. □

References

1. Almani, T., Kumar, K., Dogru, A.H., Singh, G., Wheeler, M.F.: Convergence analysis of multirate fixed-stress split iterative schemes for coupling flow with geomechanics. Comput. Methods. Appl. Mech Eng. **311**, 180–207 (2016)
2. Anderson, D.G.: Iterative procedures for nonlinear integral equations. J. ACM **12**(4), 547–560 (1965)
3. Armero, F.: Formulation and finite element implementation of a multiplicative model of coupled poro-plasticity at finite strains under fully saturated conditions. Comput. Methods. Appl. Mech. Eng. **171**(3), 205–241 (1999)
4. Bangerth, W., Kanschat, G., Heister, T., Heltai, L., Kanschat, G.: The deal.II library version 8.4. J. Numer Math. **24**, 135–141 (2016)
5. Bause, M.: Iterative coupling of mixed and discontinuous Galerkin methods for poroelasticity. In: Numerical Mathematics and Advanced Applications ENUMATH 2017, pp. 551–560. Springer International Publishing (2019)
6. Bause, M., Radu, F.A., Köcher, U.: Space–time finite element approximation of the Biot poroelasticity system with iterative coupling. Comput. Methods. Appl. Mech. Eng. **320**(Supplement C), 745–768 (2017)
7. Berger, L., Bordas, R., Kay, D., Tavener, S.: A stabilized finite element method for finite-strain three-field poroelasticity. Comput. Mech. **60**(1), 51–68 (2017)
8. Biot, M.A.: Consolidation settlement under a rectangular load distribution. J. Appl. Phys. **12**(5), 426–430 (1941)
9. Biot, M.A.: General theory of three-dimensional consolidation. J. Appl. Phys. **12**(2), 155–164 (1941)
10. Biot, M.A.: Theory of elasticity and consolidation for a porous anisotropic solid. J. Appl. Phys. **26**(2), 182–185 (1955)
11. Borregales, M., Nordbotten, J.M., Kumar, K., Radu, F.A.: Robust iterative schemes for non-linear poromechanics. Comput. Geosci. **22**(4), 1021–1038 (2017)
12. Both, J.W., Borregales, M., Nordbotten, J.M., Kumar, K., Radu, F.A.: Robust fixed stress splitting for Biot's equations in heterogeneous media. Appl. Math Lett. **68**, 101–108 (2017)
13. Both, J.W., Kumar, K., Nordbotten, J.M., Pop, I.S., Radu, F.A.: Iterative linearisation schemes for doubly degenerate parabolic equations. In: Numerical Mathematics and Advanced Applications ENUMATH 2017, pp. 49–63. Springer International Publishing, Cham (2019)
14. Both, J.W., Kumar, K., Nordbotten, J.M., Radu, F.A.: Iterative methods for coupled flow and geomechanics in unsaturated porous media. In: Proceedings of the Sixth Biot Conference on Poromechanics, vol. 68, pp. 101–108 (2017)
15. Both, J.W., Kumar, K., Nordbotten, J.M., Radu, F.A.: Anderson accelerated fixed-stress splitting schemes for consolidation of unsaturated porous media. Comput. Math. Appl. **77**(6), 1479–1502 (2019)
16. Brenner, S., Scott, R.: The Mathematical Theory of Finite Element Methods. Texts in Applied Mathematics. Springer, New York (2008). https://doi.org/10.1137/1037111
17. Brezzi, F., Fortin, M.: Mixed and Hybrid Finite Element Methods, Volume 15 of Springer Ser. Comput. Math. Springer, New York (2012)
18. Castelletto, N., White, J.A., Ferronato, M.: Scalable algorithms for three-field mixed finite element coupled poromechanics. J. Comput. Phys. **327**, 894–918 (2016)
19. Chin, L.Y., Thomas, L.K., Sylte, J.E., Pierson, R.G.: Iterative coupled analysis of geomechanics and fluid flow for rock compaction in reservoir simulation. Oil Gas Sci. Technol. **57**(5), 485–497 (2002)

20. Coussy, O.: A general theory of thermoporoelastoplasticity for saturated porous materials. Trans. Por. Med. **4**(3), 281–293 (1989)
21. Coussy, O.: Mechanics of Porous Continua. Wiley, New York (1995)
22. Coussy, O.: Poromechanics. Wiley, New York (2004)
23. Doster, F., Nordbotten, J.M.: Full Pressure Coupling for Geomechanical Multi-phase Multi-component Flow Simulations (2015)
24. Gai, X., Wheeler, M.F.: Iteratively coupled mixed and Galerkin finite element methods for poro-elasticity. Numer. Methods Partial. Diff. Equ. **23**(4), 785–797 (2007)
25. Gaspar, F.J., Rodrigo, C.: On the fixed-stress split scheme as smoother in multigrid methods for coupling flow and geomechanics. Comput. Methods Appl. Mech. Eng. **326**(Supplement C), 526–540 (2017)
26. Girault, V., Kumar, K., Wheeler, M.F.: Convergence of iterative coupling of geomechanics with flow in a fractured poroelastic medium. Comput. Geosci. **20**(5), 997–1011 (2016)
27. Hong, Q., Kraus, J., Lymbery, M., Philo, F.: Conservative discretizations and parameter-robust preconditioners for Biot and multiple-network flux-based poroelastic models. arXiv:1806.00353 (2018)
28. Hong, Q., Kraus, J., Lymbery, M., Wheeler, M.F.: Parameter-robust convergence analysis of fixed-stress split iterativemethod for multiple-permeability poroelasticity systems. arXiv:1812.11809v2 (2019)
29. Jeannin, L., Mainguy, M., Masson, R., Vidal-Gilbert, S.: Accelerating the convergence of coupled geomechanical-reservoir simulations. Int. J. Numer. Anal. Meth. Geomech. **31**(10), 1163–1181 (2007)
30. Jha, B., Juanes, R.: A locally conservative finite element framework for the simulation of coupled flow and reservoir geomechanics. Acta Geotech. **2**(3), 139–153 (2007)
31. Kim, J., Tchelepi, H.A., Juanes, R.: Stability and convergence of sequential methods for coupled flow and geomechanics. Drained and undrained splits. Comput. Methods. Appl. Mech. Eng. **200**(23–24), 2094–2116 (2011)
32. Knabner, P., Angerman, L.: Numerical Methods for Elliptic and Parabolic Partial Differential Equations, vol. 44. Springer, New York (2003)
33. Kumar, K., Pop, I., Radu, F.A.: Convergence analysis of mixed numerical schemes for reactive flow in a porous medium. SIAM J. Numer. Anal. **51**(4), 2283–2308 (2013). https://doi.org/10.1137/120880938
34. Lee, J.J., Piersanti, E., Mardal, K.-A., Rognes, M.E.: A mixed finite element method for nearly incompressible multiple-network poroelasticity. SIAM J. Sci Comput. **41**(2), A722–A747 (2018)
35. Lee, S., Mikelic, A., Wheeler, M.F., Wick, T.: Phase-field modeling of proppant-filled fractures in a poroelastic medium. Comput. Methods Appl. Mech. Eng. **312**, 509–541 (2016)
36. Lewis, R.W., Sukirman, Y.: Finite element modelling of three-phase flow in deforming saturated oil reservoirs. Int. J. Numer. Anal. Meth. Geomech. **17**(8), 577–598 (1993)
37. List, F., Radu, F.A.: A study on iterative methods for solving Richards' equation. Comput. Geosci. **20**(2), 341–353 (2016)
38. Mikelić, A., Wheeler, M.F.: Theory of the dynamic Biot-Allard equations and their link to the quasi-static Biot system. J. Math. Phys. **53**(12), 123702 (2012)
39. Mikelić, A., Wheeler, M.F.: Convergence of iterative coupling for coupled flow and geomechanics. Comput. Geosci. **18**(3–4), 325–341 (2013)
40. Nordbotten, J.M.: Stable Cell-Centered Finite Volume Discretization for Biot Equations. SIAM J. Numer. Anal. **54**(2), 942–968 (2016)
41. Pettersen, O.: Coupled Flow and Rock Mechanics Simulation Optimizing the coupling term for faster and accurate computation. Int. J. Numer. Anal. Model. **9**(3), 628–643 (2012)
42. Phillips, P.J., Wheeler, M.F.: A coupling of mixed and continuous Galerkin finite element methods for poroelasticity I: the continuous in time case. Comput. Geosci. **11**(2), 131–144 (2007)
43. Pop, I.S., Radu, F., Knabner, P.: Mixed finite elements for the Richards' equation: linearization procedure. J. Comput. Appl. Math. **168**(1–2), 365–373 (2004)
44. Prevost, J.H.: One-Way versus Two-Way Coupling in Reservoir-Geomechanical Models, pp. 517–526. American Society of Civil Engineers (2013)
45. Radu, F.A.: Mixed finite element discretization of Richards' equation: error analysis and application to realistic infiltration problems. PhD thesis. University of Erlangen–Nürnberg (2004)
46. Radu, F.A., Borregales, M., Kumar, K., Gaspar, F., Rodrigo, C.: L-scheme and Newton based solvers for a nonlinear Biot model. In: ECCOMAS Proceedings Glasgow (2018)
47. Radu, F.A., Nordbotten, J.M., Pop, I.S., Kumar, K.: A robust linearization scheme for finite volume based discretizations for simulation of two-phase flow in porous media. J. Comput. Appl. Math. **289**, 134–141 (2015)
48. Radu, F.A., Pop, I.S.: Newton method for reactive solute transport with equilibrium sorption in porous media. J. Comput. Appl. Math. **234**(7), 2118–2127 (2010)
49. Rodrigo, C., Gaspar, F.J., Hu, X., Zikatanov, L.T.: Stability and monotonicity for some discretizations of the Biot's consolidation model. Comput. Methods Appl. Mech. Eng. **298**, 183–204 (2016)
50. Rodrigo, C., Hu, X., Ohm, P., Adler, J.H., Gaspar, F.J., Zikatanov, L.: New stabilized discretizations for poroelasticity and the Stokes' equations. Comput. Methods. Appl. Mech. Eng. **341**, 467–484 (2018)
51. Settari, A., Walters, D.A.: Advances in coupled geomechanical and reservoir modeling with applications to reservoir compaction. Soc. Petrol. Eng. **6**(3) (2001)
52. Showalter, R.E.: Diffusion in poro-elastic media. J. Math Anal. Appl. **251**(1), 310–340 (2000)
53. Storvik, E., Both, J.W., Kumar, K., Nordbotten, J.M., Radu, F.A.: On the optimization of the fixed-stress splitting for Biot's equations. Int. J. Numer. Meth. Eng. **120**(2), 179–194 (2019)
54. Temam, R., Miranville, A.: Mathematical Modeling in Continuum Mechanics. Cambridge (2005)
55. Wan, J., Durlofsky, L.J., Hughes, T.J.R., Aziz, K.: Stabilized Finite Element Methods for Coupled Geomechanics - Reservoir Flow Simulations (2003)
56. White, D., Ganis, B., Liu, R., Wheeler, M.F.: Near-Wellbore study with a Drucker-Prager plasticity model coupled with a parallel compositional reservoir simulator. In: Paper SPE-182627-MS SPE Reservoir Simulation Conference (2017)
57. Yi, S.-Y., Bean, M.L.: Iteratively coupled solution strategies for a four-field mixed finite element method for poroelasticity. Int. J. Numer. Anal. Methods Geomech. **41**(2), 159–179 (2016)
58. Zienkiewicz, O.C., Paul, D.K., Chan, A.H.C.: Unconditionally stable staggered solution procedure for soil-pore fluid interaction problems. Int. J. Numer. Meth. Eng. **26**(5), 1039–1055 (1988)